Electronic Supplementary Material (ESI) for Analytical Methods.

Supporting Information

3D darkfield imaging and single particle tracking of peptide-coated nanocargoes in cell

Hui Shen, Bin Xiong, Ruili Xu, Xiaodong Cheng, Yan He* and Edward S. Yeung

State Key Laboratory of Chemo/Biosensing and Chemometrics, College of Chemistry and Chemical Engineering, College of Biology, Hunan University, Changsha, 410082, P. R. China.

SUPPLEMENTARY EXPERIMENTAL SECTION

Chemicals. Mercaptosuccinic acid (MSA), N-(3-Dimethylaminopropyl)-N-ethylcarbodiimide hydrochloride crystalline (EDC), 2-(N-Morpholino)ethanesulfonic acid (MES), N-Hydroxysulfosuccinimide sodium salt (Sulfo-NHS) were obtained from Sigma-Aldrich (USA). All other reagents were AR grade and were purchased from Sinopharm Chemical Reagent (Shanghai, China). Deionized (DI) water was obtained using a Milli-Q system.

AuNPs Preparation and Surface Modification of AuNPs. The first step in 3D dark-field imaging is to synthesize high quality monodispersed AuNPs. In order to suppress the scattering intensity of cellular components that contribute to the optical background and interference, which requires the size of AuNPs to be generally larger than 80 nm,[1] we chose a seed-mediated growth method to synthesize large AuNPs.[2] First, seed AuNPs were prepared by the Frens method.[3] Briefly, 1.03 mL of 2.428×10^{-2} M $HAuCl_4$ was gently mixed with 98.97 mL DI water

and then the mixture was heated to boil for 5 min. Then 0.588 mL of 0.2 M sodium citrate solution was rapidly injected into the boiling solution all at once. The mixture was vigorously stirred and refluxed for 30 min. After the color of the mixture was changed to wine red, the colloidal solution was cooled by stirring at room temperature for another 15 min. The seed AuNPs prepared by this protocol have an average size of ~18 nm. After that, 300 μL of the seed AuNPs were added into 40.0 mL of DI H_2O at room temperature, and then 990 μL of 2.428×10^{-2} M $HAuCl_4$ was also added into the solution. After thorough mixing, 1440 μL of 0.01 M MSA solution (prepared in NaOH solution) was added into the mixture sequentially. The reaction was finished in about 2 h and the colloidal solution was stored at room temperature.

To modify the AuNPs with cell penetrating peptide (CPP) from the HIV-1 protein Tat (sequence: CALNN-YGRKKRRQRRR, Apeptide, Shanghai, China) via EDC/NHS chemistry,[4] 0.01 M EDC and 0.01 M sulfo-NHS stock solutions were first prepared in 0.01 M MES buffer solution (pH =5.5). CPP was dissolved in 0.01 M PB buffer (pH =7.4) at 2.0 mg/mL. 2 mL of 60 pM of the as-prepared AuNP solution was centrifuged and resuspended in 1.0 mL MES buffer. To activate the AuNP surface −COOH groups, 200 μL EDC and 50μL sulfo-NHS were added to the solution and shaked for 30 min at room temperature. The mixture was washed via centrifugation and the precipitate was dispersed to 1mL PB buffer. Subsequently, 50 μL CPP was added to the solution and the solution was shaked gently at room temperature for another 24 h. The CPP-modified AuNPs (CPP-AuNPs) were obtained by centrifugation and resuspended in PB buffer and stored at 4℃. The as-prepared AuNPs and CPP-AuNPs were characterized with a UV-Vis spectrometer (Shimadzu UV-1800, Japan), a transmission electron microscope (JEM 1230, JEOL, Japan) and a Nano ZS instrument (Malvern Instruments, UK). The size distribution was measured from TEM images by counting more than 500 nanoparticles.

3D Darkfield Imaging System. 3D darkfield imaging and tracking were performed on a 80i upright microscope (Nikon, Japan) equipped with an oil-immersion darkfield condenser (NA 1.20-1.43) and a 60X Plan Fluor objective. It was modified to be able to perform 3D imaging by incorporation of a cylindrical lens (1,000 mm focal length). Images and movies were collected by using a Neo sCMOS Camera (Andor, UK) and recorded with an exposure time of 50 ms and frame rate of 13 Hz. A motorized rotational stage (SGSP-40YAM, Sigma Koki, Japan) was coupled to the fine adjustment knob of the microscope to precisely control the stage position along the z-direction with step size of 0.69 nm. It is known that the depth of field can be calculated according to the formula: $d = \frac{\lambda n}{NA^2} + \frac{n}{M \times NA} \times e$, where λ is the wavelength of the light in air, n is the refractive index of the medium, e is the pixel size of the CCD camera and M is the magnification of the objective. Here, λ is taken to be 613 nm, which is the LSPR maximum of the CPP-AuNP probe, n=1.518 for oil, e=6.5 μm and M=60. Thus, d is 2.134 μm.

Cell Culture and Imaging. The cervical cancer HeLa cell lines were obtained from American Type Cell Culture (ATCC, USA). The cells were cultured on a coverslip placed in a plastic culture dish and maintained in high DMEM (Dulbecco's Modified Eagle's medium with high glucose, GIBCO) supplemented with 10% fetal bovine serum (GIBCO) at 37℃ and 5% CO_2 in a humidified atmosphere. After the cells reaching 70-80% confluency, 50 μL CPP-AuNPs (see the Supporting Information for detailed preparation method) were added into the petri dish and incubated with the cells for 30 min. Before the observation, we replaced the culture medium by phenol-red-free DMEM to reduce the optical absorption of the medium and improve the contrast of images. For tracking of individual particles, the coverslip was rinsed with the culture medium three times and put upside-down on a glass slide with a concavity filled with the culture medium. The observation lasts for at least 30 min. Determination of the w_x and w_y, and the position of the centroid x_0 and y_0 of the particle was performed using custom scripts written in Matlab

(Mathworks, USA). And the codes for visualization of the 3D color-coded trajectories was written in Matlab and was gratefully provided by Dr. Sripad Ram. Post-processing of the collected images and movies, as well as data analysis and visualization were performed using ImageJ (NIH, USA).

SUPPLEMENTARY RESULTS AND DISCUSSIONS

AuNP Characterization. As shown in the TEM image (Figure S1A), the as-prepared AuNPs were mostly spherical with uniform sizes. Statistical analysis showed that their average size was 127.9±14.1 nm (Figure S1B). The AuNPs were modified with CPP because CPP is supposed to be an efficient ligand to improve active internalization of nanoparticles into the cell.[5] Figure S1C shows the UV-Vis spectra of freshly prepared AuNPs and the ones after CPP-modification. The latter red-shifted from 597 nm to 613 nm with obvious band broadening. The spectral shift can be attributed to the formation of a CPP layer on the surface of the AuNPs, which changed the local charge distribution and the relative permittivity of the particle.[6] Figure S1D shows hydrodynamic diameter distribution of the AuNPs; after CPP modification, their average diameter increased slightly from 130 nm to 145 nm. In addition, the zeta potential measurements indicated that the surface charge of the AuNPs increased from -29.0 mV (excess carboxyl groups) to 27.2 mV (positive charge of the Tat peptide) after the modification of CPP, further confirming that the CPP was successfully modified on the AuNPs surface.

Overview of 3D Imaging Technqiues. During the past, several different techniques towards fluorescence-based 3D SPT have been advanced from 2D imaging methods for the purpose of achieving some axial resolution.[7, 8] The first demonstration was based on the use of a cylindrical lens in the optical path to create an asymmetry above and below the average focal plane, allowing the axial position of the fluorophore to be coded in the ratio of x and y widths of the

detected 2D PSF.[9] And with this approach, 3D super-resolution STORM imaging of photoswitchable cyanine dyes has been accomplished successfully, with an axial accuracy of 22 nm.[10] A second method was developed by recording the signal of a single molecule in distinct different focal planes simultaneously.[11] With this multi-focal detection approach, the z position of a molecule could be determined with an accuracy of 14.4 nm over 2.5 μm axially in 3D SPT of QD-labeled transferrin receptor in a live cell.[12] However, because of the complexity of the multi-camera setup, this approach is only applicable to a few planes. Moreover, the determination of distance between the two focal planes in the object space and the lateral magnifications can lead to biased z-position estimates. A third method relied on PSF engineering that uses a spatial light modulator (SLM) to engineer a double-helix point spread function (DH-PSF) that has two rotating lobes, where the angle of rotation depends on the z-position of the emitting molecule.[13] With DH-PSF based 3D fluorescence microscopy, a 10-20 nm localization accuracy along the z direction was achieved, allowing investigation the dynamics of a specific mRNA in living yeast cells.[14] This successful method, however, suffers from the considerable technology complexity to manufacture a liquid crystal SLM; moreover, the efficiency of photon collection was so low that it currently can only be applied to a specific number of high quantum yield fluorescent dyes or proteins.[14-16] Another less commonly used method is interferometry measurement, which integrates a single-photon multiphase interferometric scheme with PALM,[17] and the output beams from 3-way beam splitter were used to determine the axial position of the source molecule. It achieved sub-20 nm accuracy with fluorescent nanoparticles, but it remained limited to fixed samples. In all these methods, the astigmatism method is especially appealing because of its simplicity, which introduces a clear distinction between positions above and below the focal plane. Even though this approach has several practical limitations such as its applicability only at certain depth, it is straightforward enough to simply place a cylindrical lens

in the detection path, which can be implemented in any standard light microscope. So, we chose the astigmatism method to achieve 3D SPT.

The z Position Calibration. In order to get the z coordinates from the x- and y- widths of the single particle images, a calibration curve was generated. Calibration data were collected using CCP-AuNPs by immobilizing them on the coverslip surface at a low density to ensure that every individual particle is well-separated. To change the z position of the sample during collection of calibration data, the motorized rotational stage was raised in steps of 0.138 μm. For the calibration, images of individual particles were acquired at a series of z positions, which were specified relative to the average focal plane (z=0). The acquired particle images were then subjected to weighted overdetermined regression analysis[18] via 2D elliptical Gaussian fitting

$$I_{xy} = A \cdot exp(-\frac{(x - x_0)^2}{2 \cdot w_x^{\,2}} - \frac{(y - y_0)^2}{2 \cdot w_y^{\,2}}) + \varepsilon_{xy} \qquad (1)$$

where I_{xy} is the intensity of the image, A is the peak amplitude, x_0 and y_0 are the position of the centroid, and w_x and w_y stand for the width of PSF in x and y direction, respectively. Determination of the w_x and w_y of the particle was performed using custom scripts written in Matlab. Thus, the variation of the measured w_x and w_y as a function of recorded z position according to the motorized rotational stage could be obtained. The calibration curve was then generated by fitting to a modified form of a typical defocusing curve[10]. In this work, the calibration curve in Figure 1B was constructed from the average w_x and w_y values of eight individual AuNPs at each z position. To determine the z coordinate of another particle, its measured w_x and w_y values were compared with the calibration curve by minimizing the distance

$$D = \sqrt{(\mathrm{w}_x - \mathrm{w}_{x,\mathrm{fit}})^2 + (\mathrm{w}_y - \mathrm{w}_{y,\mathrm{fit}})^2} \qquad (2)$$

The z coordinate that corresponds to the minimum distance was chosen as the true coordinate. This procedure allowed the z coordinate of each CPP-AuNP to be obtained.

Analysis of the motion of the particle. Single particle trajectories were analyzed using an approach similar to that described by Saxton and Jacobson[19] with the exception that the particle motion was extended to 3D instead of 2D. Briefly, the trajectory of each particle can be analyzed from its mean square displacement (MSD) as a function of lag time t. For random diffusion, particles moving with a single 3D diffusion coefficient (D) can be described by

$$MSD = 6Dt \tag{3}$$

In the case of directed diffusion, a drift velocity v is superimposed on random diffusion

$$MSD = 6Dt + v^2t^2 \tag{4}$$

These models were fitted to the experimental data to obtain D and v for the particles.

SUPPLEMENTARY MOVIES

Movie 1. Complex 3D trafficking itinerary of a CPP-AuNP undergoing endocytosis. The movie corresponds to Figure 2A and the CPP-AuNP of interest is indicated by a red arrow.

SUPPERLENTARY FIGURES AND CAPTIONS

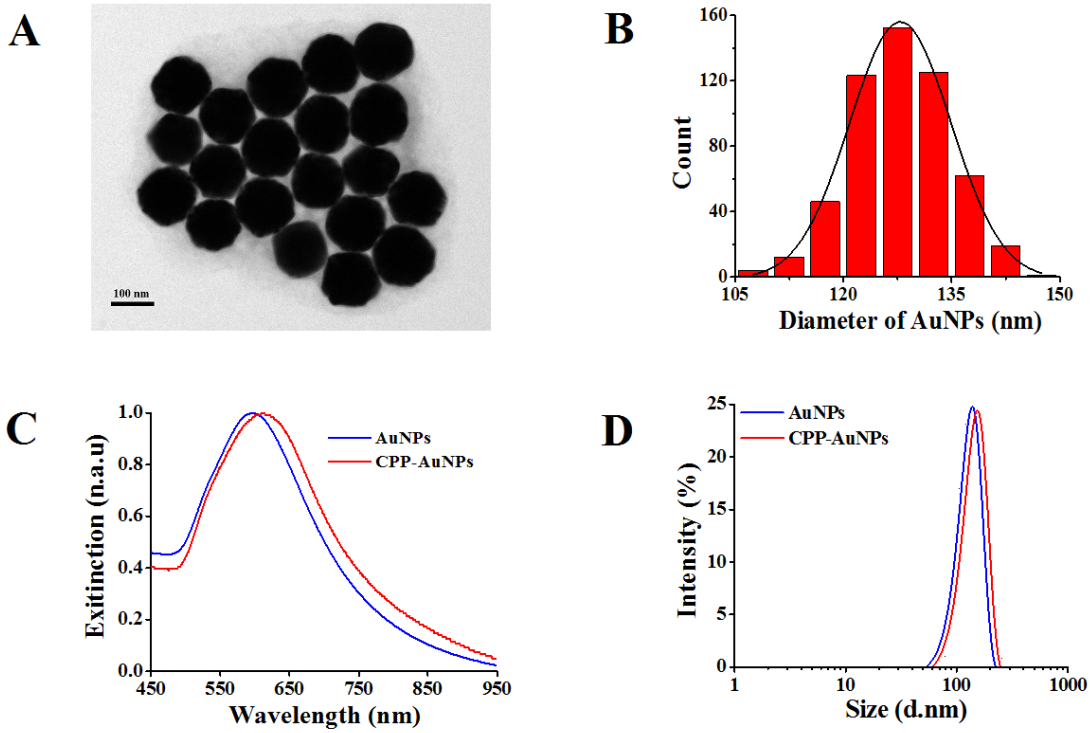

Figure S1. AuNP characterizations. (A) Typical TEM image and (B) size distribution of the as-prepared AuNPs. Over 540 particles were counted. (C) UV-Vis spectra and (D) DLS results of the AuNPs before and after CPP modification.

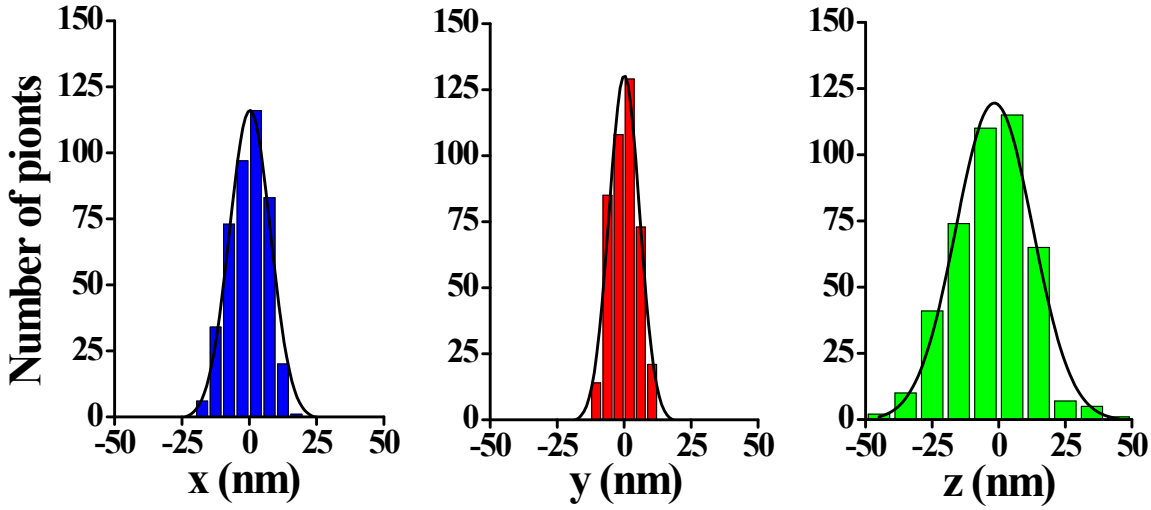

Figure S2. Histograms of all distributions in x-, y-, and z-axes. The standard deviations of these distributions quantifying the localization precision are: σ_x=15.2±0.7 nm, σ_y=11.4±0.5 nm and σ_z=28.9±2.6 nm.

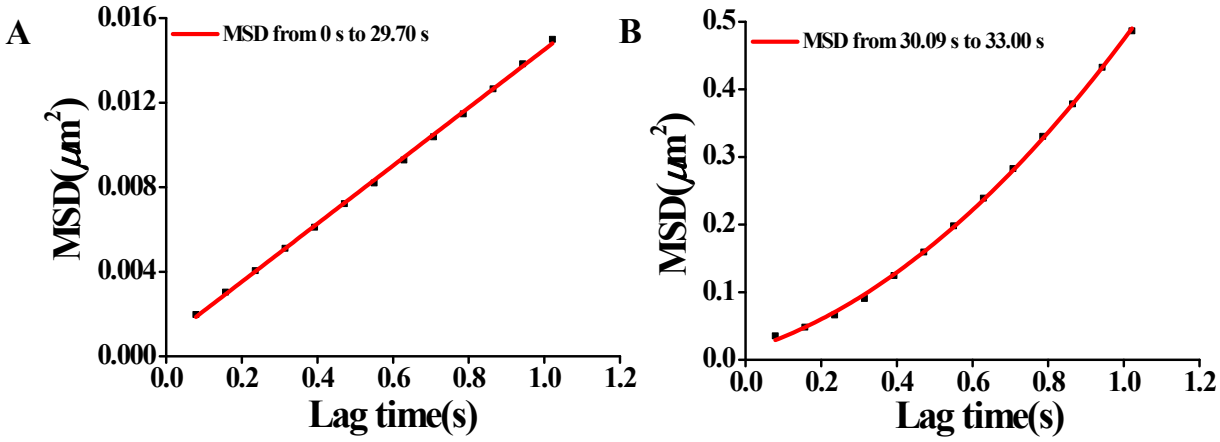

Figure S3. (A) The measured MSD of particle P1as a function of lag time T during its diffusion on the plasma membrane (black). The red line is a fit to equation 3 with D= 0.002 μm^2/s. (B) The MSD analysis of the P1 trajectory after its internalization. The red curve is a fit to equation 4 with D= 0.03 μm^2/s and v= 0.5 μm/s. The upward-bending of the MSD is characteristic for directional active transport of the particle inside the cell.

REFERENCES

1. L. Xiao, L. Wei, X. Cheng, Y. He and E. S. Yeung, *Anal. Chem.*, 2011, **83**, 7340-7347.
2. J. Niu, T. Zhu and Z. Liu, *Nanotechnology*, 2007, **18**, 325607.
3. G. Frens, *Nature*, 1973, **241**, 20-22.
4. D. Bartczak and A. G. Kanaras, *Langmuir*, 2011, **27**, 10119-10123.
5. M. C. Morris, S. Deshayes, F. Heitz and G. Divita, *Biol. Cell*, 2008, **100**, 201-217.
6. R. Lévy, N. T. K. Thanh, R. C. Doty, I. Hussain, R. J. Nichols, D. J. Schiffrin, M. Brust and D. G. Fernig, *J. Am. Chem. Soc.*, 2004, **126**, 10076-10084.
7. A. S. Stender, K. Marchuk, C. Liu, S. Sander, M. W. Meyer, E. A. Smith, B. Neupane, G. Wang, J. Li, J.-X. Cheng, B. Huang and N. Fang, *Chem. Rev.*, 2013, **113**, 2469-2527.
8. A. Dupont and D. C. Lamb, *Nanoscale*, 2011, **3**, 4532-4541.
9. H. P. Kao and A. S. Verkman, *Biophys. J.*, 1994, **67**, 1291-1300.
10. B. Huang, W. Wang, M. Bates and X. Zhuang, *Science*, 2008, **319**, 810-813.
11. M. F. Juette, T. J. Gould, M. D. Lessard, M. J. Mlodzianoski, B. S. Nagpure, B. T. Bennett, S. T. Hess and J. Bewersdorf, *Nat. Methods*, 2008, **5**, 527-529.
12. S. Ram, P. Prabhat, J. Chao, E. S. Ward and R. J. Ober, *Biophys. J.*, 2008, **95**, 6025-6043.
13. S. R. P. Pavani, M. A. Thompson, J. S. Biteen, S. J. Lord, N. Liu, R. J. Twieg, R. Piestun and W. E. Moerner, *Proc. Natl. Acad. Sci. U. S. A.*, 2009, **106**, 2995-2999.
14. M. A. Thompson, J. M. Casolari, M. Badieirostami, P. O. Brown and W. E. Moerner, *Proc. Natl. Acad. Sci. U. S. A.*, 2010, **107**, 17864-17871.
15. M. A. Thompson, M. D. Lew, M. Badieirostami and W. E. Moerner, *Nano Lett.*, 2010, **10**, 211-218.
16. M. P. Backlund, M. D. Lew, A. S. Backer, S. J. Sahl, G. Grover, A. Agrawal, R. Piestun and W. E. Moerner, *Proc. Natl. Acad. Sci. U. S. A.*, 2012, **109**, 19087-19092.
17. G. Shtengel, J. A. Galbraith, C. G. Galbraith, J. Lippincott-Schwartz, J. M. Gillette, S. Manley, R. Sougrat, C. M. Waterman, P. Kanchanawong, M. W. Davidson, R. D. Fetter and H. F. Hess, *Proc. Natl. Acad. Sci. U. S. A.*, 2009, **106**, 3125-3130.
18. S. M. Anthony and S. Granick, *Langmuir*, 2009, **25**, 8152-8160.
19. M. J. Saxton and K. Jacobson, *Annu. Rev. Biophys. Biomol. Struct.*, 1997, **26**, 373-399.